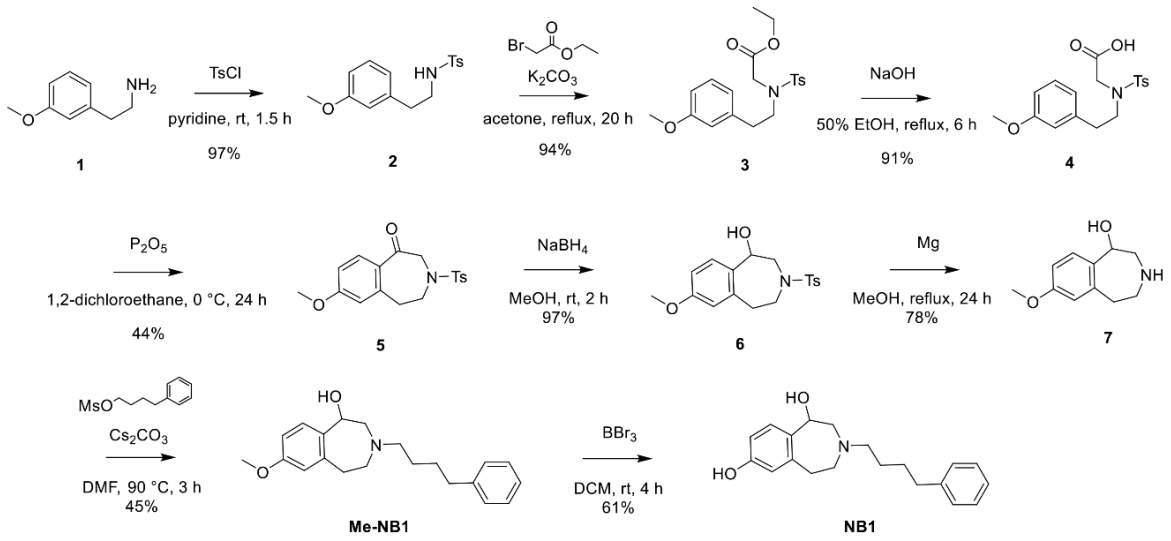

Supplemental Figure 1: Synthesis of reference compound **Me-NB1** and of the phenolic precursor **NB1** .

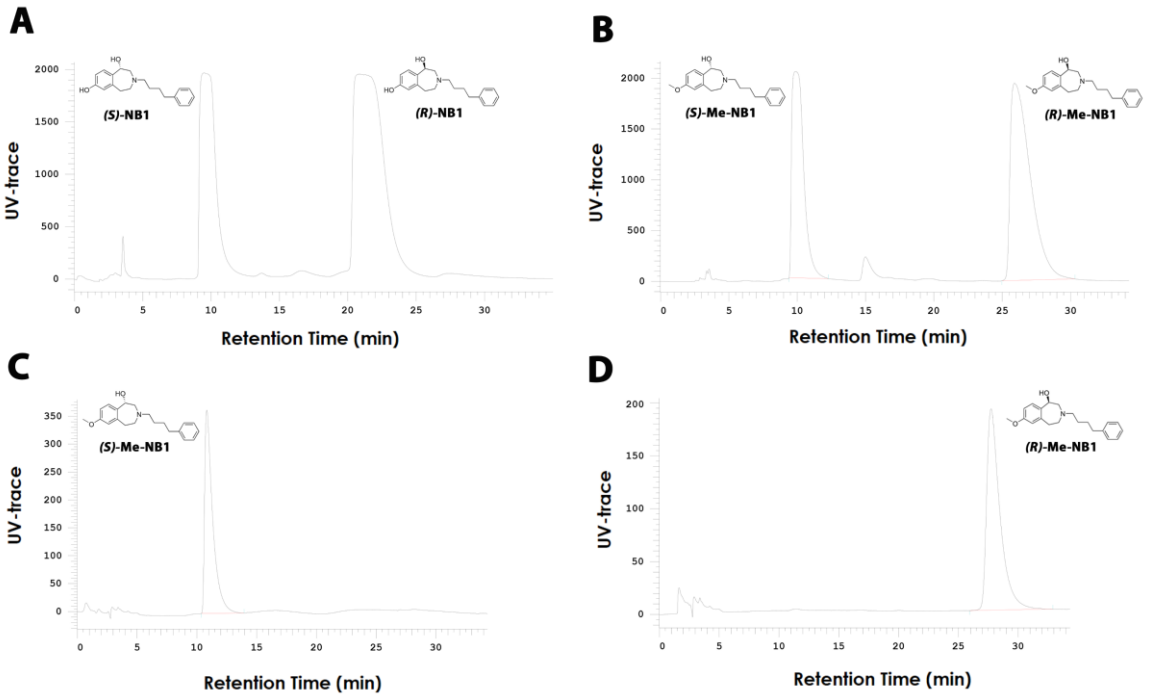

Supplemental Figure 2: Chiral HPLC separation of Me-NB1 and NB1 under isocratic normal phase conditions (hexane/isopropanol 8:2). **A.** Semipreparative chromatogram after chiral resolution of *(rac)*-NB1. **C.** Semipreparative chromatogram after chiral resolution of *(rac)*-Me-NB1. **C.** Quality control of *(S)*-Me-NB1 **D.** Quality control of *(R)*-Me-NB1.

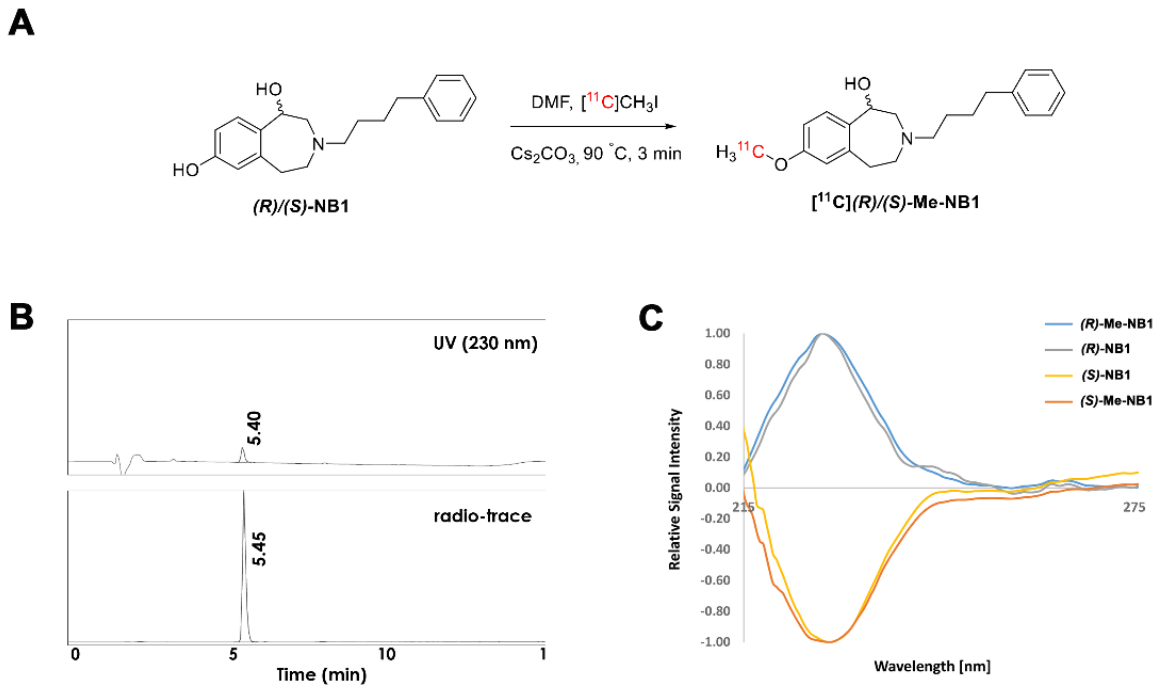

Supplemental Figure 3: A. Radiolabeling of ***(R)*- and *(S)*-^{11}C-Me-NB1** was achieved by treatment of the phenolic precursor in analogy to the procedure recently published by our group . **B.** Quality control of formulated tracer by UV- and radio-trace. **C**. Circular dichroism spectra recorded in the range between 215 – 275 nm for *(R)*-Me-NB1, *(S)*-Me-NB1, *(R)*-NB1 and *(S)*-NB1.

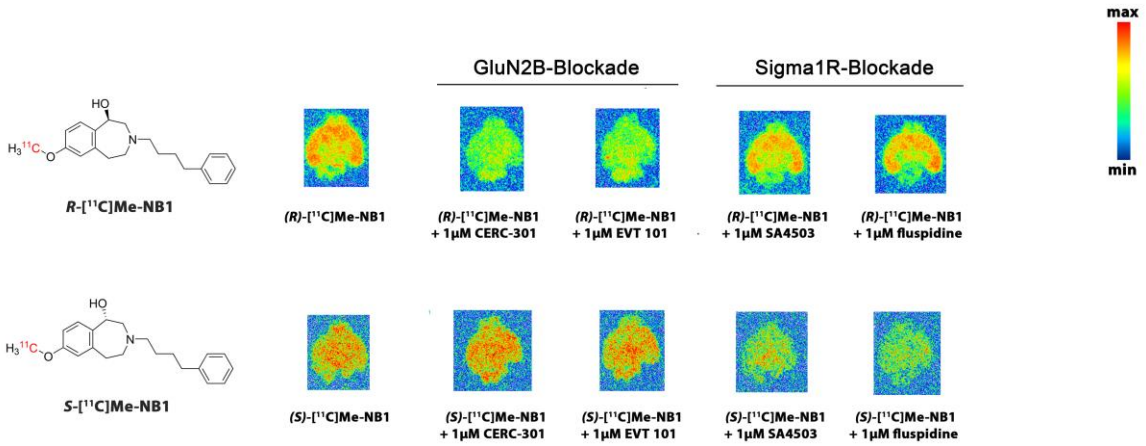

Supplemental Figure 4: Representative autoradiograms of *(R)*-^{11}C-Me-NB1 and *(S)*-^{11}C-Me-NB1 on coronal mouse brain sections. The binding of *(R)*-^{11}C-Me-NB1 was heterogeneous and GluN2B-specific while *(S)*-^{11}C-Me-NB1 showed considerable σ_1R binding. The blocking studies revealed selectivity of the *R*-enantiomer over σ_1R. In contrast, the *S*-enantiomer exhibited considerable binding to the σ_1 receptor.

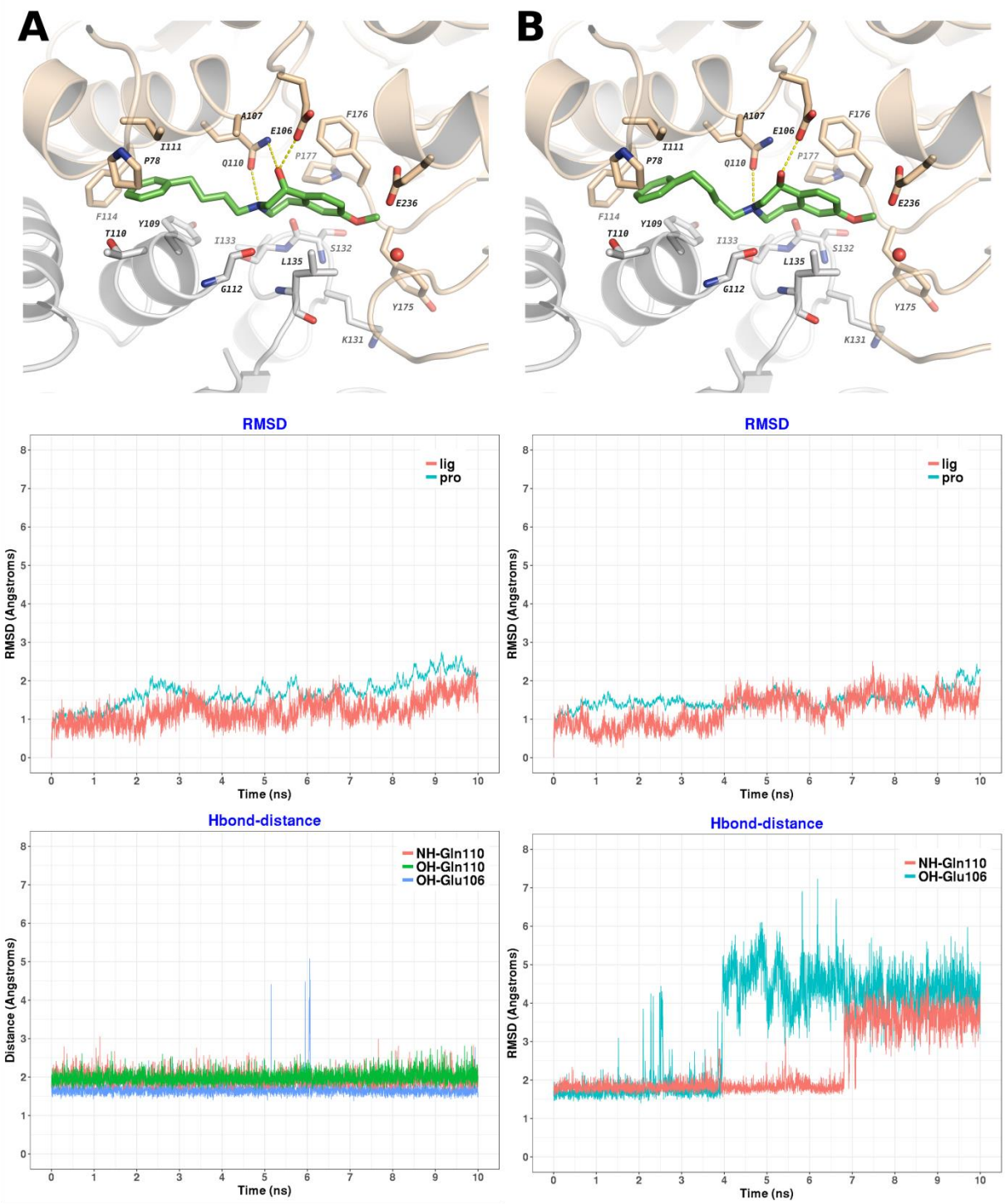

Supplemental Figure 5: Molecular dynamics simulation of the most stable *(R)*-Me-NB1 and *(S)*-Me-NB1 binding modes and stability of the predicted hydrogen-bond interactions. **A**. *(R)*-Me-NB1 interactions were observed between the ligand NH-group and glutamine 110 as well as the ligand OH-group and both glutamate 106 and glutamine 110 of the GluN2B subunit. Hydrogen bonds were maintained during MD. **B**. *(S)*-Me-NB1 interactions were observed between the ligand NH-group and glutamine 110

as well as the ligand OH-group and glutamate 106. No interaction between ligand OH-group and glutamine 110 was predicted. Hydrogen bonds were not maintained during MD.

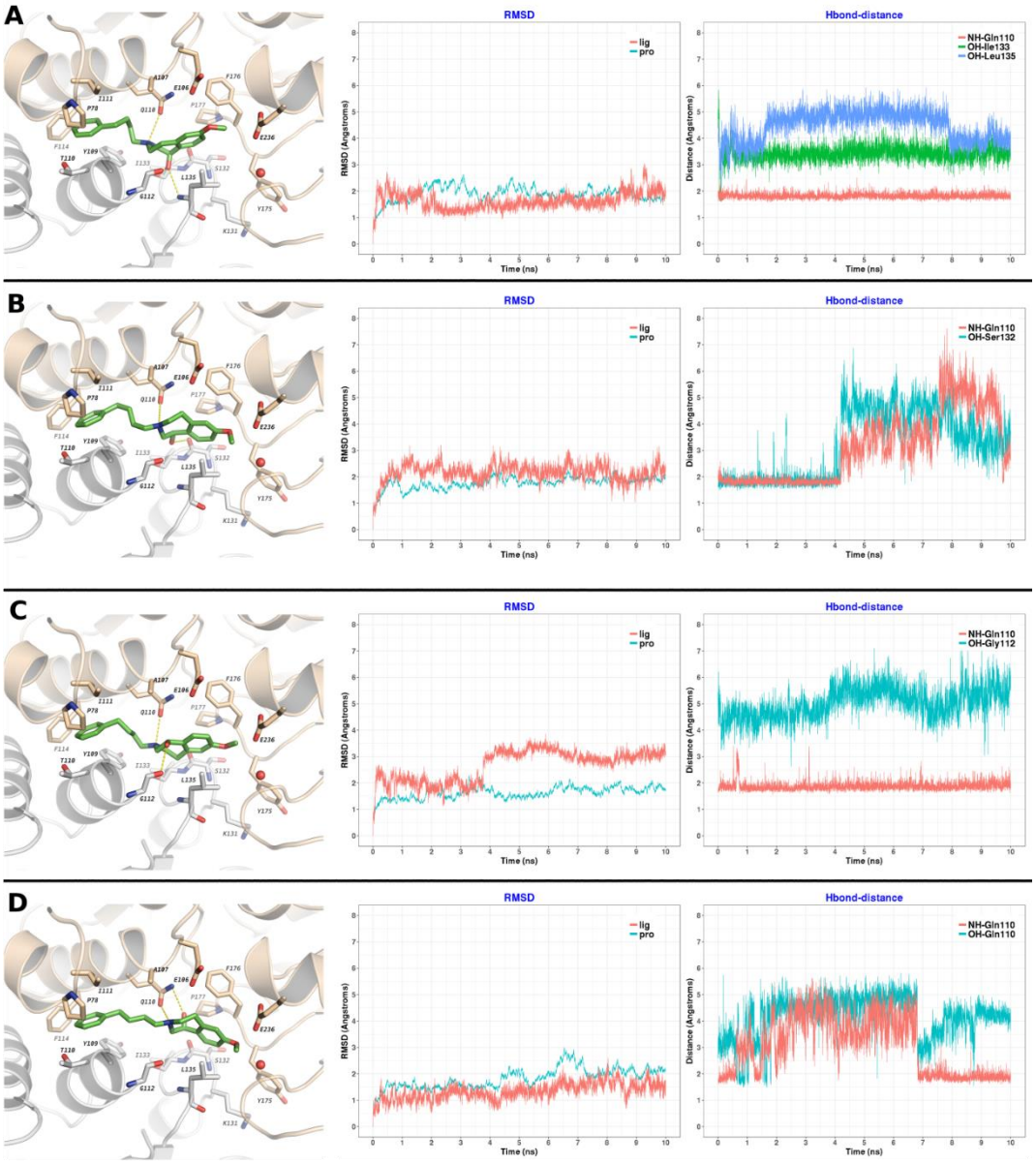

Supplemental Figure 6: Molecular dynamics simulation of the less stable binding modes of ***(R)*-Me-NB1** (**A** and **B**) and ***(S)*-Me-NB1** (**C** and **D**).

Supplemental Table 1: Calculated MM-GBSA binding free energies (kcal/mol) for the two most stable ***(R)-*** and ***(S)*-Me-NB1** binding modes using different GB models. Standard error of the mean (SEM) is given in brackets.

	GB1	**GB2**	**GB5**	**GB8**
***(R)*-Me-NB1**	-59.99 (0.43)	-56.38 (0.44)	-60.56 (0.47)	-51.61 (0.58)
***(S)*-Me-NB1**	-54.90 (0.53)	-49.57 (0.53)	-53.71 (0.56)	-39.04 (0.78)

A

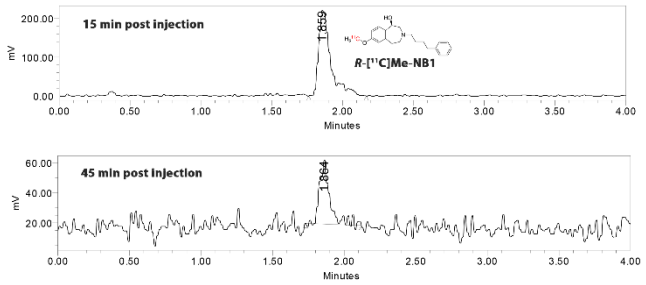

B

Brain

Time (min)	*(R)*- [^{11}C]Me-NB1 (%)	metabolites (%)
0	100	0
15	100	0
45	100	0

Plasma

Time (min)	*(R)*- [^{11}C]Me-NB1 (%)	metabolites (%)
0	100	0
5	79.5	20.5
15	57.5	42.5
45	42.2	57.8

Supplemental Figure 7: Metabolite study with *(R)*-^{11}C-Me-NB1 was performed in male Wistar rats. **A**. Radio-UPLC analysis of the brain samples after 15 and 45 min post injection revealed the presence of parent tracer. No radiometabolite was detected. **B**. Radio-TLC analysis confirmed the radio-UPLC findings for the brain samples. Plasma data at 45 min post injection indicate that 42.0% of the intact parent was still present.

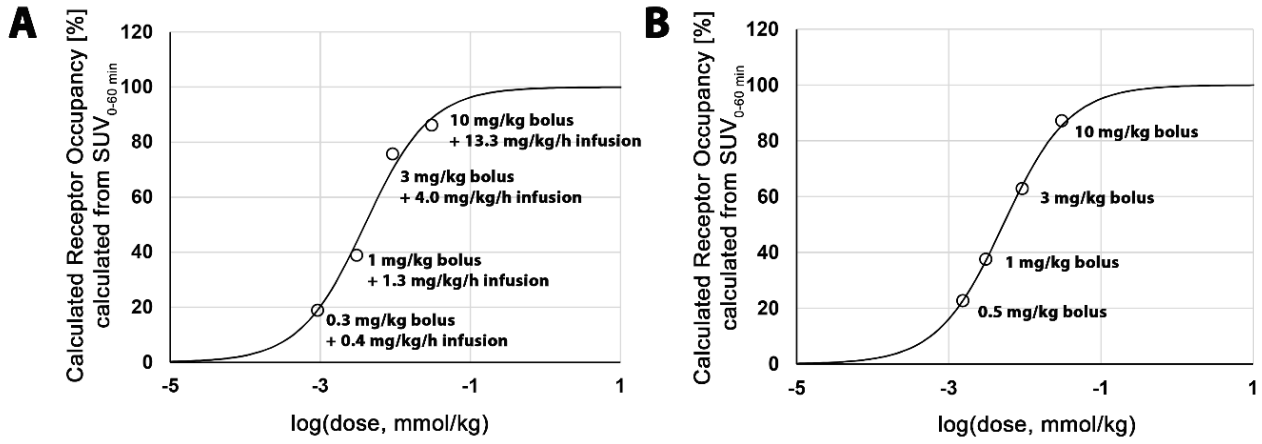

Supplemental Figure 8: Receptor occupancy studies with *(R)*-^{11}C-Me-NB1 and GluN2B-antagonist CP101,606 in male Wistar rats. **A**. Target occupancy was studied upon bolus injections, followed by infusion of CP101,606 to maintain constant plasma levels. **B**. Target occupancy was studied upon bolus injection only, without further infusion of CP101,606. The following equations were used to calculate receptor occupancies: AUC = (bmax - bmin) * D_{50}/(D + D_{50}) + bmin; RO = (bmax - AUC)/(bmax - bmin) * 100, where AUC is the area under the curve of the respective PET scan, D_{50} is the dose required for 50 % receptor occupancy, D is the actual dose, RO is the receptor occupancy in % and bmax as well as bmin are the maximum and minimum binding, respectively.

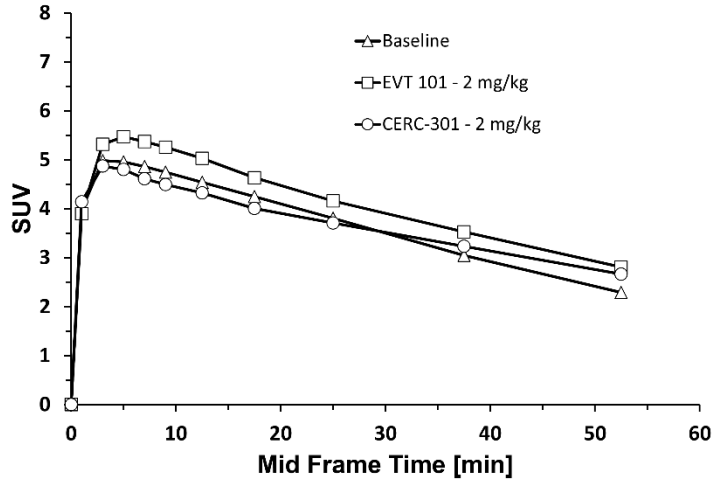

Supplemental Figure 9: PET experiments with *(R)*-^{11}C-Me-NB1 and GluN2B-antagonist CERC-301 and EVT 101 as blocking agents. No blocking effect was observed for the dose of 2 mg/kg, suggesting the lack of *in vivo* target engagement.

Organ	*5 min p.i.*	*15 min p.i.*	*15 min p.i + eliprodil 2 mg/kg*	*30 min p.i.*	*45 min p.i.*	*60 min p.i.*
spleen	0.180 ± 0.014	0.329 ± 0.076	0.290 ± 0.030	0.296 ± 0.030	0.266 ± 0.030	0.196 ± 0.029
liver	0.119 ± 0.015	0.147 ± 0.022	0.146 ± 0.006	0.146 ± 0.013	0.184 ± 0.007	0.176 ± 0.029
kidney	0.588 ± 0.125	0.480 ± 0.019	0.203 ± 0.022	0.378 ± 0.043	0.339 ± 0.041	0.251 ± 0.028
adrenal gland	0.600 ± 0.215	1.597 ± 0.335	0.542 ± 0.045	1.400 ± 0.232	1.344 ± 0.283	1.468 ± 0.395
lung	1.100 ± 0.196	0.479 ± 0.167	0.464 ± 0.061	0.299 ± 0.042	0.220 ± 0.078	0.155 ± 0.028
femur	0.057 ± 0.014	0.068 ± 0.004	0.076 ± 0.010	0.086 ± 0.006	0.083 ± 0.004	0.070 ± 0.014
heart	0.163 ± 0.007	0.086 ± 0.016	0.099 ± 0.008	0.054 ± 0.004	0.050 ± 0.008	0.037 ± 0.003
fat	0.012 ± 0.003	0.035 ± 0.022	0.046 ± 0.009	0.039 ± 0.010	0.048 ± 0.006	0.046 ± 0.009
intestine	0.126 ± 0.008	0.223 ± 0.051	0.305 ± 0.037	0.390 ± 0.069	0.544 ± 0.057	0.521 ± 0.027
testicle	0.041 ± 0.011	0.071 ± 0.017	0.072 ± 0.008	0.092 ± 0.009	0.102 ± 0.011	0.108 ± 0.010
blood	0.022 ± 0.002	0.017 ± 0.002	0.025 ± 0.003	0.015 ± 0.009	0.017 ± 0.000	0.016 ± 0.000
urine	0.043 ± 0.017	0.065 ± 0.022	0.140 ± 0.073	0.141 ± 0.001	0.150 ± 0.053	0.195 ± 0.071
muscle	0.090 ± 0.007	0.074 ± 0.019	0.076 ± 0.006	0.065 ± 0.096	0.057 ± 0.007	0.040 ± 0.004
pancreas	0.487 ± 0.136	0.775 ± 0.170	0.221 ± 0.029	0.766 ± 0.007	0.715 ± 0.055	0.627 ± 0.031
skin	0.030 ± 0.005	0.035 ± 0.007	0.048 ± 0.002	0.054 ± 0.160	0.051 ± 0.005	0.057 ± 0.010
brain	0.353 ± 0.052	0.292 ± 0.040	0.189 ± 0.023	0.256 ± 0.024	0.210 ± 0.018	0.169 ± 0.014

Supplemental Table 2: Organ biodistribution of *(R)*-^{11}C-Me-NB1 in Wistar rats (n=4), reported as averaged % normalized injected dose per gram body weight ± standard deviation. Twenty-four male Wistar rats were tail-vein injected with *(R)*-^{11}C-Me-NB1 (13 – 30 MBq, 0.5 – 4.9 nmol/kg) and sacrificed by decapitation under isoflurane anaesthesia (induced 5 min before decapitation) at the time points 5, 15, 30, 45 and 60 min p.i. (n = 4 for every time point). Additionally, a blockade study was conducted by injection of 2 mg/kg eliprodil in an aqueous vehicle of pH 7.0 containing glucose (5 %), NaCl (0.45 %) and citric acid (1 mM) shortly before the radiotracer and rats have been euthanized at 15 min post injection. The same vehicle was injected into baseline animals shortly before tracer administration. Organs were dissected, weighed and the radioactivity was measured with a gamma-counter. Results were reported as % normalized injected dose per gram organ.

Brain region	*5 min p.i.*	*15 min p.i.*	*15 min p.i + eliprodil 2 mg/kg*	*30 min p.i.*	*45 min p.i.*	*60 min p.i.*
olfactory bulb	0.327 ± 0.039	0.242 ± 0.033	0.149 ± 0.017	0.206 ± 0.018	0.173 ± 0.014	0.135 ± 0.004
hippocampus	0.291 ± 0.053	0.250 ± 0.039	0.192 ± 0.021	0.236 ± 0.019	0.213 ± 0.020	0.174 ± 0.017
thalamus	0.337 ± 0.046	0.304 ± 0.039	0.212 ± 0.024	0.271 ± 0.032	0.221 ± 0.019	0.176 ± 0.016
cerebellum	0.292 ± 0.048	0.248 ± 0.027	0.175 ± 0.025	0.204 ± 0.020	0.158 ± 0.014	0.129 ± 0.011
brain stem	0.275 ± 0.035	0.260 ± 0.038	0.173 ± 0.019	0.266 ± 0.022	0.239 ± 0.018	0.213 ± 0.025
midbrain	0.322 ± 0.045	0.294 ± 0.048	0.187 ± 0.021	0.282 ± 0.026	0.236 ± 0.019	0.195 ± 0.020
cortex	0.430 ± 0.063	0.329 ± 0.048	0.198 ± 0.024	0.273 ± 0.026	0.218 ± 0.018	0.164 ± 0.011
restbrain	0.225 ± 0.035	0.229 ± 0.036	0.177 ± 0.030	0.216 ± 0.016	0.200 ± 0.022	0.183 ± 0.028
striatum	0.360 ± 0.072	0.306 ± 0.053	0.200 ± 0.025	0.253 ± 0.026	0.202 ± 0.011	0.155 ± 0.013

Supplemental Table 3: Regional biodistribution of *(R)*-^{11}C-Me-NB1 in the Wistar rat brain (n=4), reported as averaged % normalized injected dose per gram body weight ± standard deviation.